Monitoring Ground Deformation at the Aquistore CO_2 Storage Site with RADARSAT-2 DInSAR

G41A-0467

(1) Sergey Samsonov, (1) Magdalena Czarnogorska, (2) Don White, (3) Michael Craymer

(1) Canada Centre for Mapping and Earth Observation, NRCan, Ottawa, ON, Canada, email: sergey.samsonov@nrcan-rncan.gc.ca (2) Geological Survey of Canada, NRCan, Ottawa, ON, Canada (3) Geodetic Survey Division, NRCan, Ottawa, ON, Canada

ABSTRACT: The research objectives of the Aquistore CO_2 storage project are to design, adapt, and test non-seismic monitoring methods for measurement, and verification of CO_2 storage, and to integrate data to determine subsurface fluid distributions, pressure changes and associated surface deformation. The test area is located west of the Boundary Dam Power Station in southeastern Saskatchewan, Canada. The targeted CO_2 injection zones are within the Winnipeg and Deadwood formations located at > 3000 m depth. For measuring background (prior to CO_2 injection) ground deformation at this site we employed the advanced satellite Differential Interferometric Synthetic Aperture Radar (DInSAR) Multidimensional Small Baseline Subset (MSBAS) technique. DInSAR-MSBAS results were calculated based on eighty RADARSAT-2 images from four different ascending and descending beams acquired during 2012-2014. We detected slow ground deformation with a rate of up to 1 cm/year not related to CO_2 injection but caused by different natural and anthropogenic causes. We discuss in detail DInSAR-MSBAS processing chain and analyze precision of derived deformation rates and time series.

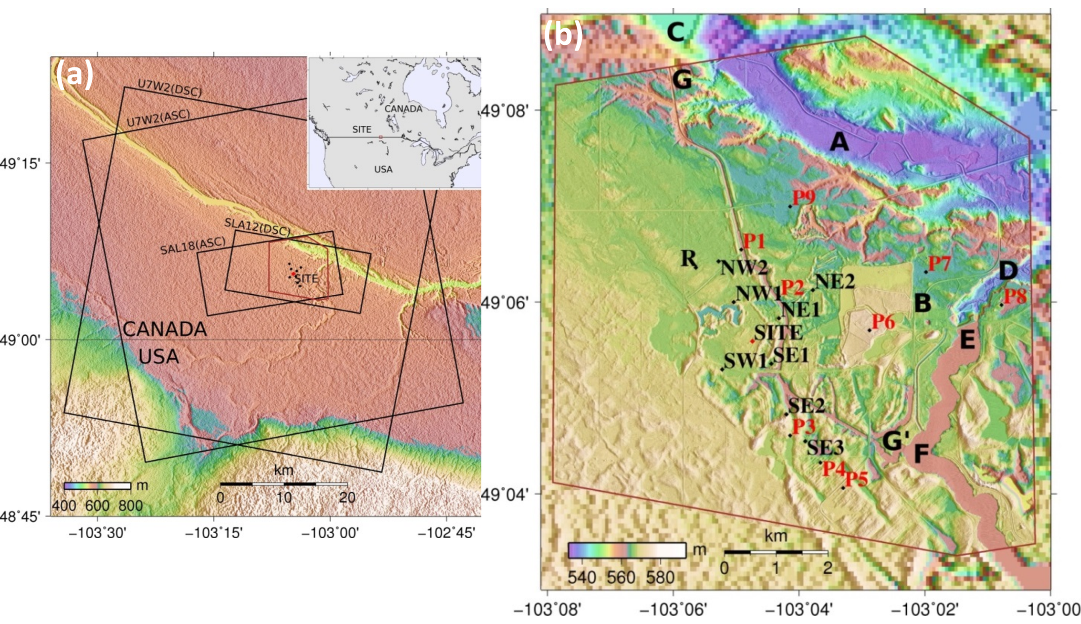

LOCATION

Aquistore project study area, southeastern Saskatchewan: (a) ASTER 30 m resolution Digital Elevation Model (DEM) (USGS/gdex, 2014). RADARSAT-2 frames are outlined in black. Region of interest is outlined in brown. (b) LIDAR 1m resolution DEM plotted over ASTER DEM. Reference region "R" assumed to be as stable. Monitoring sites with corner reflectors installed NE1, NE2, SE1, SE2, SE3, SITE, SW1, NW1, NW2 are plotted in black. Points P1-P9 experiencing fast ground deformation are plotted in red. Location of injection site is plotted as red diamond. A - Souris river, B - Boundary Dam Power Station, C – Rafferty Dam, D - Long Creek river, E - Boundary Dam, F - Boundary Dam Reservoir, GG' - Rafferty-Boundary diversion canal.

SATELLITE DATA AND PROCESSING METHODOLOGY

For monitoring ground deformation at the Aquistore storage site we used DInSAR (Differential Synthetic Aperture Radar Interferometry) (Massonnet and Feigl, 1998; Rosen et al., 2000) advanced MSBAS (Multidimensional Small Baseline Subset) (Samsonov et al, 2011; Samsonov et al. 2012) processing technique that computes the two dimensional (2D), vertical and horizontal, deformation time series by combing SAR data from various sensors and acquisition geometries, therefore significantly improving overall temporal resolution. To achieve high temporal and high spatial resolution of deformation measurements SAR data from four high resolution ascending and descending RADARSAT-2 beams, Spotlight and Wide Ultra-Fine, was acquired. By using four independent beams the temporal resolution was increased by a factor of four from 24 to six days, allowing detection of transient signals with minimal delay. High coherence is necessary for an accurate phase unwrapping. A single master for each beam was selected and remaining slave images were co-registered and re-sampled to the master geometry. Topographic phase was computed from the 1 m resolution air-borne LIDAR Digital Elevation Model (DEM) and removed from the interferograms. Adaptive filtering (Goldstein and Werner, 1998), phase unwrapping (Costantini, 1998) and geocoding procedures were applied. The residual orbital ramps were computed and removed. The MSBAS technique was applied in order to produce vertical and horizontal East-West deformation rates and time series.

Table shows SAR datasets used in the study area

RADARSAT-2 Spotlight 18 (SLA18), Spotlight 12 (SLA12), Wide 2 Ultra-Fine 7 (U7W2); time span (in YYYYMMDD format), range-azimuth resolution, range-azimuth multilooking, azimuth and incidence angles Φ, number of available SAR images N, and number of calculated interferograms M for each dataset

InSAR set	Time span	SLC resolution (rg-az)	Multilooking (rg-az)	Θ [°]	Φ [°]	N	M
R2 SLA18 (asc)	20120605-20140923	1.6-0.8	3-12	351	44	25	184
R2 SLA12 (dsc)	20120716-20140916	1.6-0.8	3-12	-170	40	20	156
R2 U7W2 (asc)	20120619-20140820	1.6-2.8	4-3	349	37	18	110
R2 U7W2 (dsc)	20120615-20141003	1.6-2.8	4-3	-170	37	17	81
Total	**20120605-20141003**					**80**	**531**

Graphs show temporal and spatial baselines of RADARSAT-2 interferograms used in the study. Overall 80 SAR images spanning 20120605-20141003 produced 531 interferograms with perpendicular baselines less than 400m.

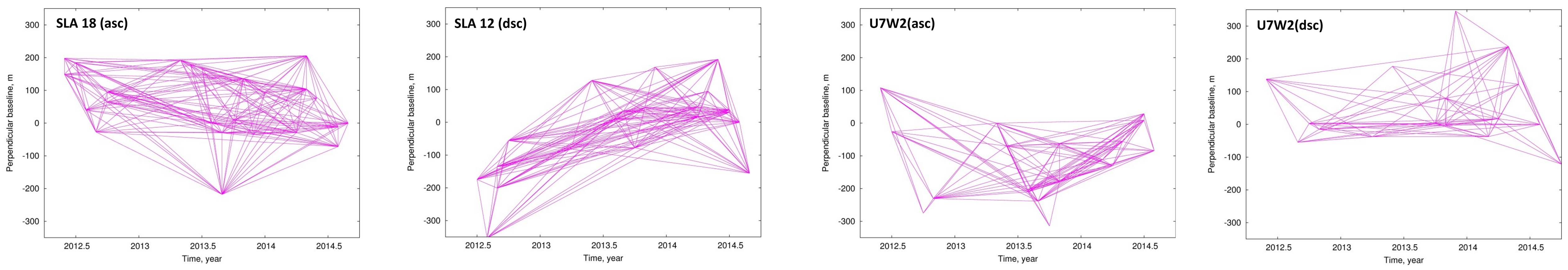

SIMULATED GROUND DEFORMATION DUE TO CO_2 INJECTION

Modelling was performed in order to simulate ground deformation that would be produced by CO2 injection with the rate of 0.5 ML/year to the depth d of 3500 m. We assumed that the density of CO2 is equal to 1000 kg/m3 (e.g. Nordbotten et al., 2005), therefore, 0.5 ML/year is equal to 0.5 MT/year. An elastic point pressure source (i.e. Mogi model) was assumed to be located at the injection depth (Mogi, 1958; Tiampo et al., 2000; Dzurisin, 2006; Samsonov et al., 2010). The increase in pressure resulted in surface deformation shown in figures (a) and (b) below. The vertical component shows uplift or heave with the maximum magnitude of about 1 cm/year centered above the injection well. The horizontal component shows zero motion above the injection well that increases with a distance from the well and reaches its maximum of about 0.5 cm/year at d/√2 or about 2475 m away from the injection well. The location of the maximum horizontal deformation is marked with the red dashed circle in figure (b). Vertical deformation component is larger than horizontal within the blue circle with radius d. Horizontal signal displays linear symmetry, which may not be clear in figure (b) due to particular colour palette. Monitoring sites and reference region "R" are plotted in black.

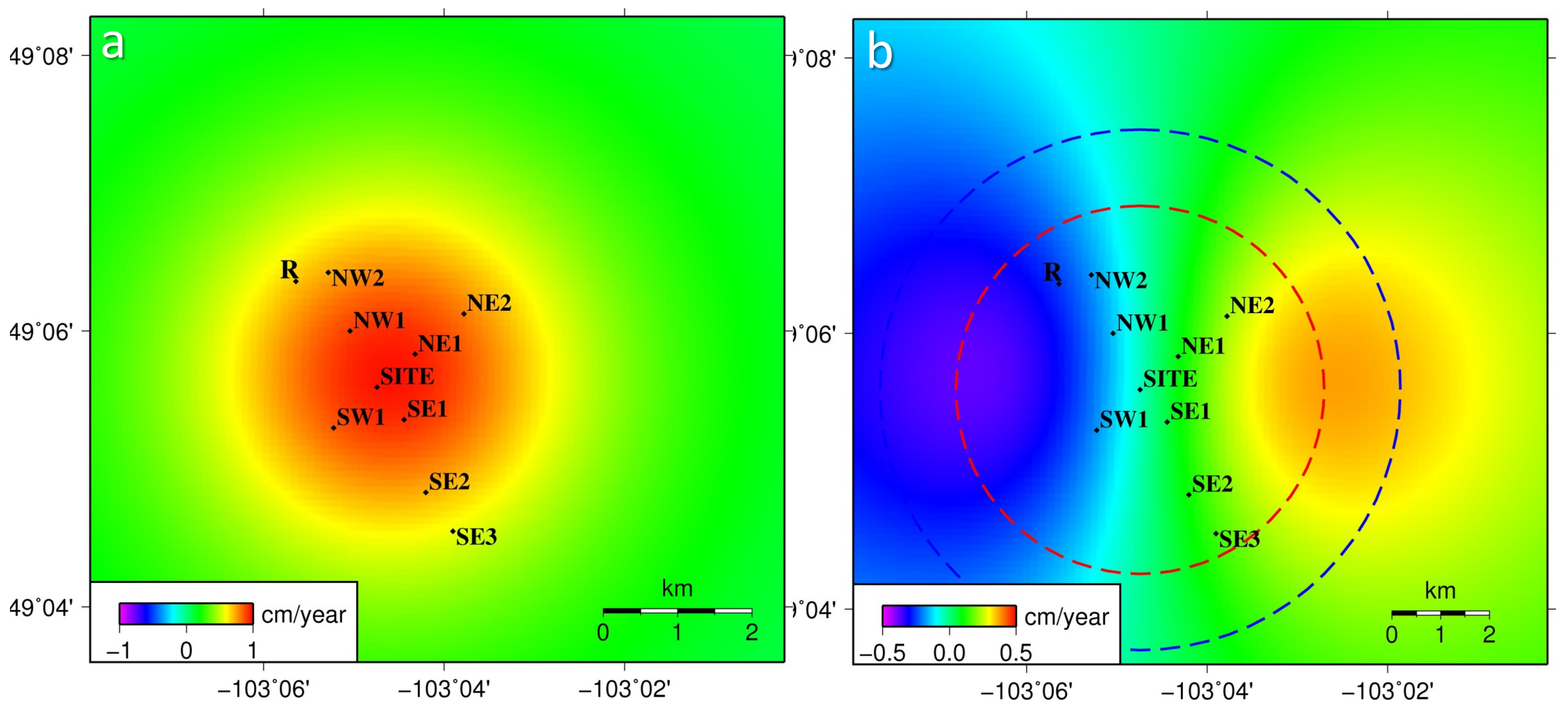

Modeled vertical (c) and horizontal (East-West) (d) deformation rates superimposed on observed MSBAS deformation rates. Presented here signal is expected in case of CO2 injection. Monitoring sites and reference region "R" are plotted in black. In (d) red circle marks region where horizontal displacements produced by injection reach maximum. Blue circle marks region at which vertical and horizontal displacements produced by injection are equal.

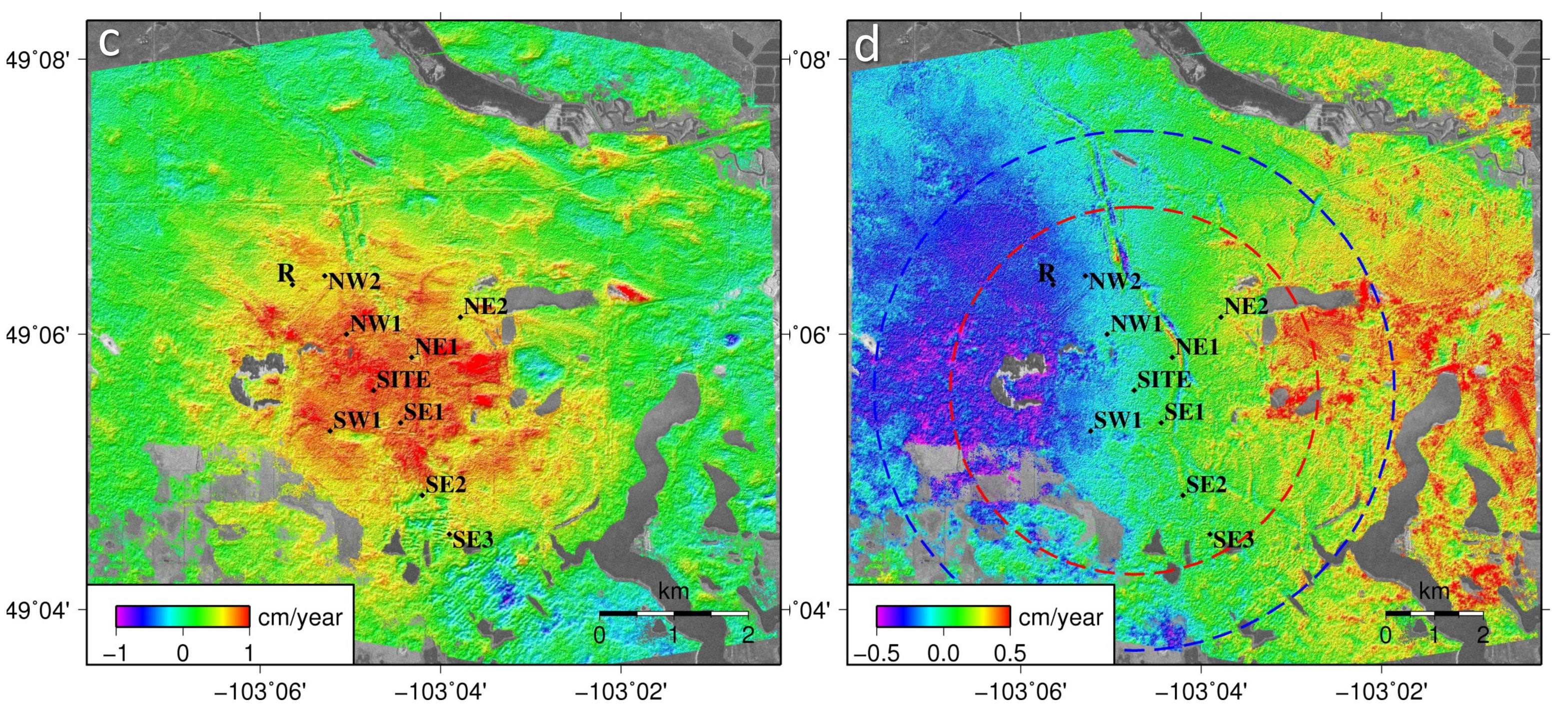

VERTICAL (IN RED) AND HORIZONTAL (IN GREEN) (EAST-WEST) MSBAS TIME SERIES OF GROUND DEFORMATION FOR MONITORING SITES NE1, NE2, SE1, SE2, SE3, SITE, SW1, NW1, NW2 COMPUTED BY MSBAS METHOD FROM RADARSAT-2 DATA. SIMULATED TIME SERIES (MARKED AS "SIM") DUE TO CONTINUOUS CO_2 INJECTION AND BACKGROUND PROCESSES ARE PLOTTED IN LIGHT RED AND LIGHT GREEN.

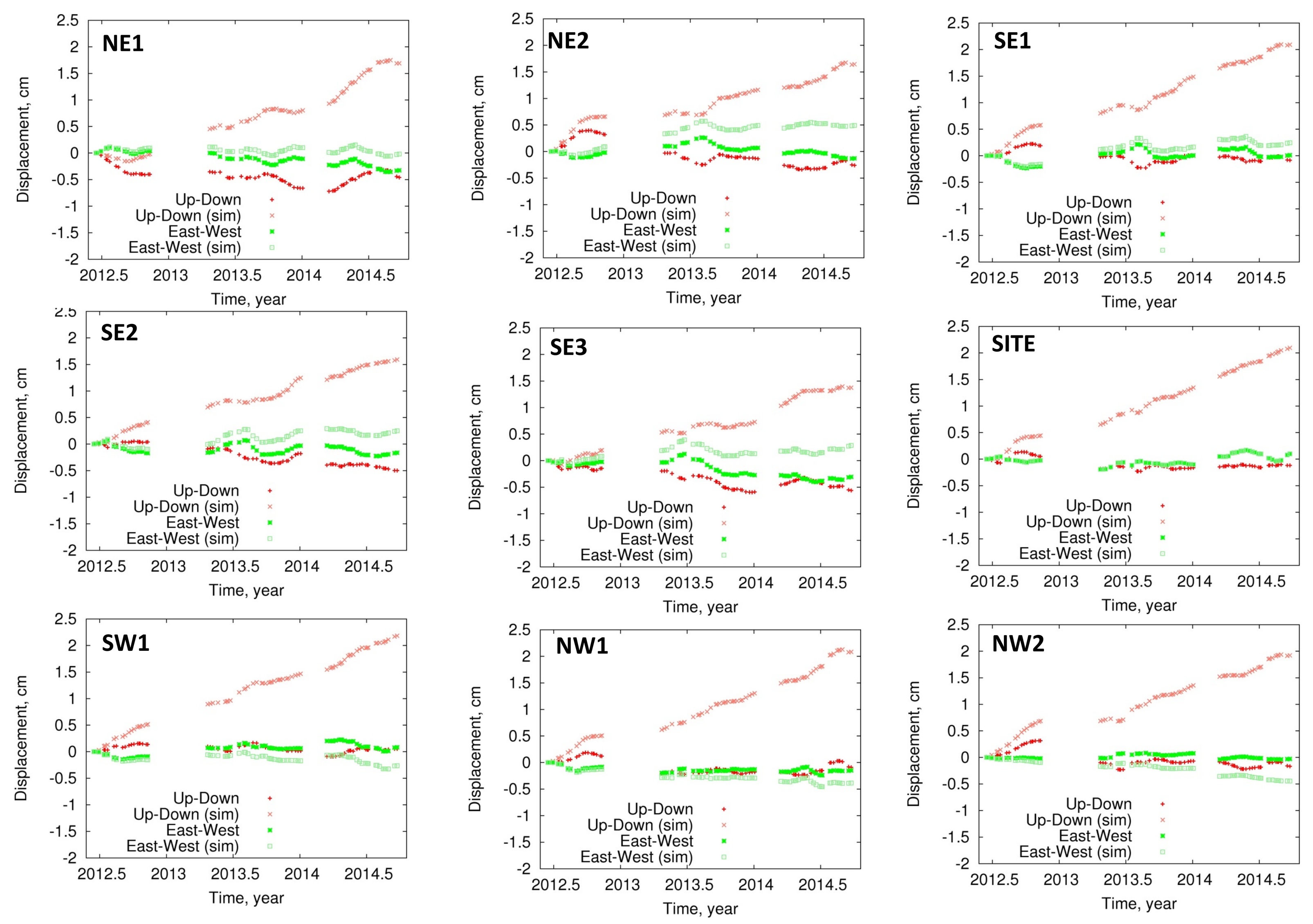

OBSERVED MSBAS GROUND DEFORMATION PRIOR TO CO_2 INJECTION

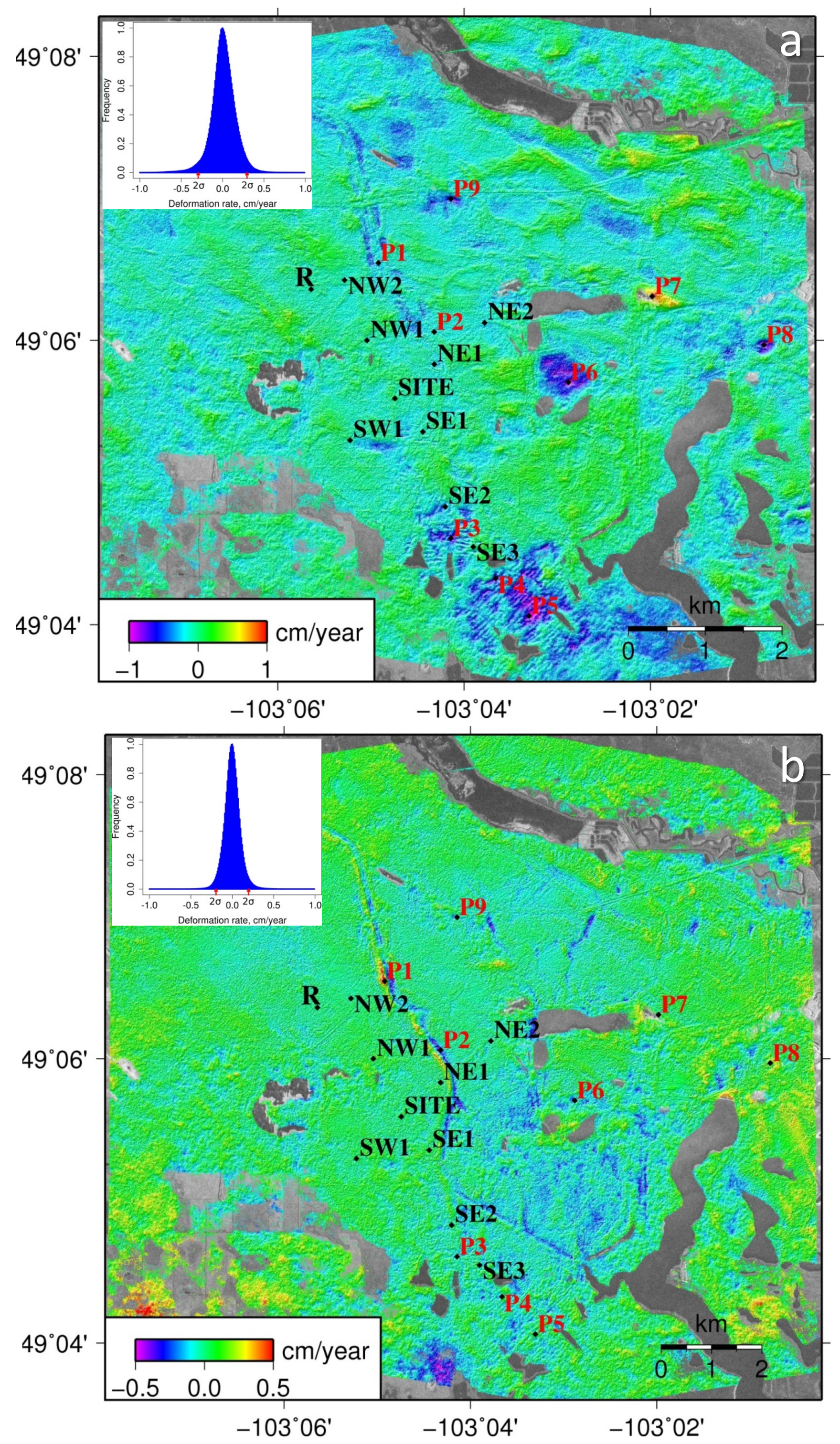

VERTICAL (IN RED) AND HORIZONTAL (IN GREEN) TIME SERIES OF GROUND DEFORMATION FOR SELECTED REGIONS P1-P9 EXPERIENCING FAST GROUND DEFORMATION COMPUTED BY MSBAS METHOD FROM RADARSAT-2 DATA

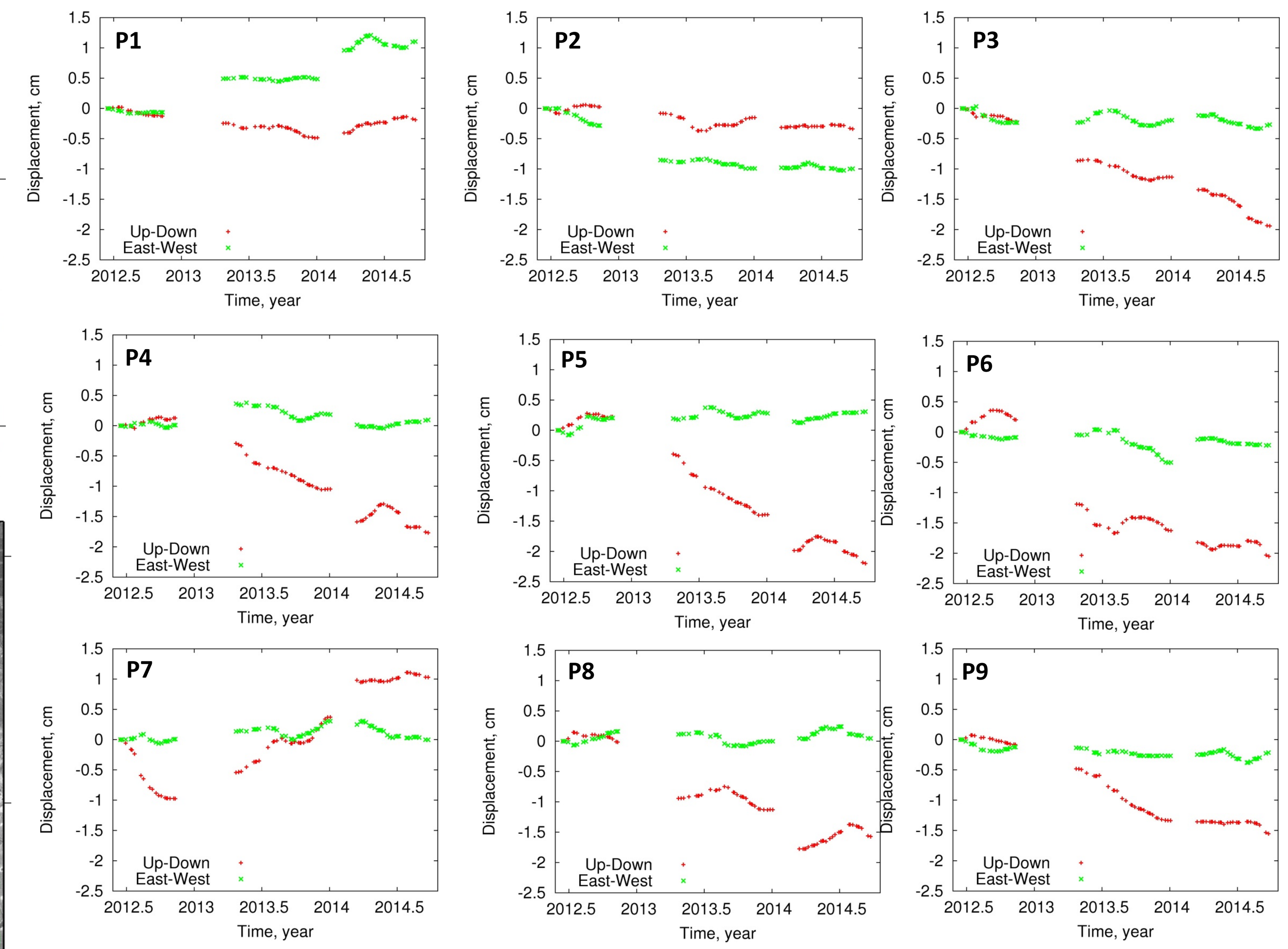

Observed vertical up to ±1 cm/year (a) and horizontal East-West up to ±0.5 cm/year (b) MSBAS deformation maps for 20120605-20141003 time span. Monitoring sites and reference region "R" are plotted in black. Points P1-P9 experiencing fast ground deformation are plotted in red. SAR intensity image is exposed in background in regions of low coherence. Histograms of vertical (a) and horizontal E-W (b) distribution of deformation rates are added to the maps. Red arrows mark 2σ 95% confidence interval equal to 0.3 cm/year and 0.2 cm/year respectively. Deformation time series were reconstructed from the deformation rates and mean deformation rate was computed by fitting a line to time series. The actual time series show stable condition with moderate seasonal variability. We computed many highly coherent small-baseline interferograms achieving nearly uniform temporal coverage throughout the year, except during winter.

CONCLUSIONS:

Satellite interferometry or DInSAR can be successfully used for detecting ground deformation at the carbon sequestration studies, prior, during and after CO_2 injection. SAR data from multiple satellites and acquisition geometries can be combined together to produce deformation time series with high temporal sampling. In this study we achieved 0.2-0.3 cm/year measurement precision and about 6 days sampling rate by combining four RADARSAT-2 beams with the individual repeat cycle of 24 days. We achieved five meter spatial resolution over about 8x8 km area. In order to accurately map deformation due to CO_2 injection the background deformation need to be estimated first. In this case we found that two years of observations are sufficient to map background processes with high-precision. The deformation rate maps for the Aquistore storage site showed active ground deformation prior to CO_2 injection. Vertical ground deformation with the maximum rate of ±1 cm/year are caused by natural and anthropogenic processed, such as, erosion, groundwater withdrawal and recharge, and post-mining activities. Horizontal motion with the maximum rate of ±0.5 cm/year is caused by erosion of the man-made structures. Large number of SAR images acquired during June 2012-October 2014 allowed computing many highly coherent small-baseline interferograms achieving nearly uniform temporal coverage throughout the year, except during winter. Nine paired (i.e. ascending-descending) corner reflectors were installed at monitoring sites along with continuous GPS, tiltmeters, and gravimeters. Forward modeling based on Mogi elastic pressurized point source model determined that extent of deformation due to injection is very broad. While the maximum of vertical component is located at the injection well, the maximum of horizontal component is located 2475 m away from the injection well. This means that the current location of the monitoring sites is sub-optimal. While vertical motion is accurately mapped at sites SITE, NE1, SE1, SW1, NW1. The horizontal motion at these sites is very small. The sites NE2, SE2, SE3, SW2, NW2 would capture signal better if they were removed from the injection well by 2475 m. In case of 2D MSBAS solution presented here the maximum East-West displacement would be observed along the East-West direction, while in case of 3D continuous GPS North-South components will also be well resolved along the North-South direction.

SURFICIAL GEOLOGY

Study area is strongly affected by different kind of glaciofluvial processes as well as anthropogenic changes due to mining activity and man-made structures. Concerning the surficial geological map, the majority of the area is located in the morainal eroded by glacial melt streams (infomaps.gov.sk.ca, 2014). In the area there are many small waterbodies and some of them are intermittent after snow melting. DInSAR heave is registered in the North-East part, heaving zone lays elongated with the Souris river morphology where the main geological environment is alluvial floodplain. But also mining exploitation was performed there in historical time and post mining works are carried out nowadays.

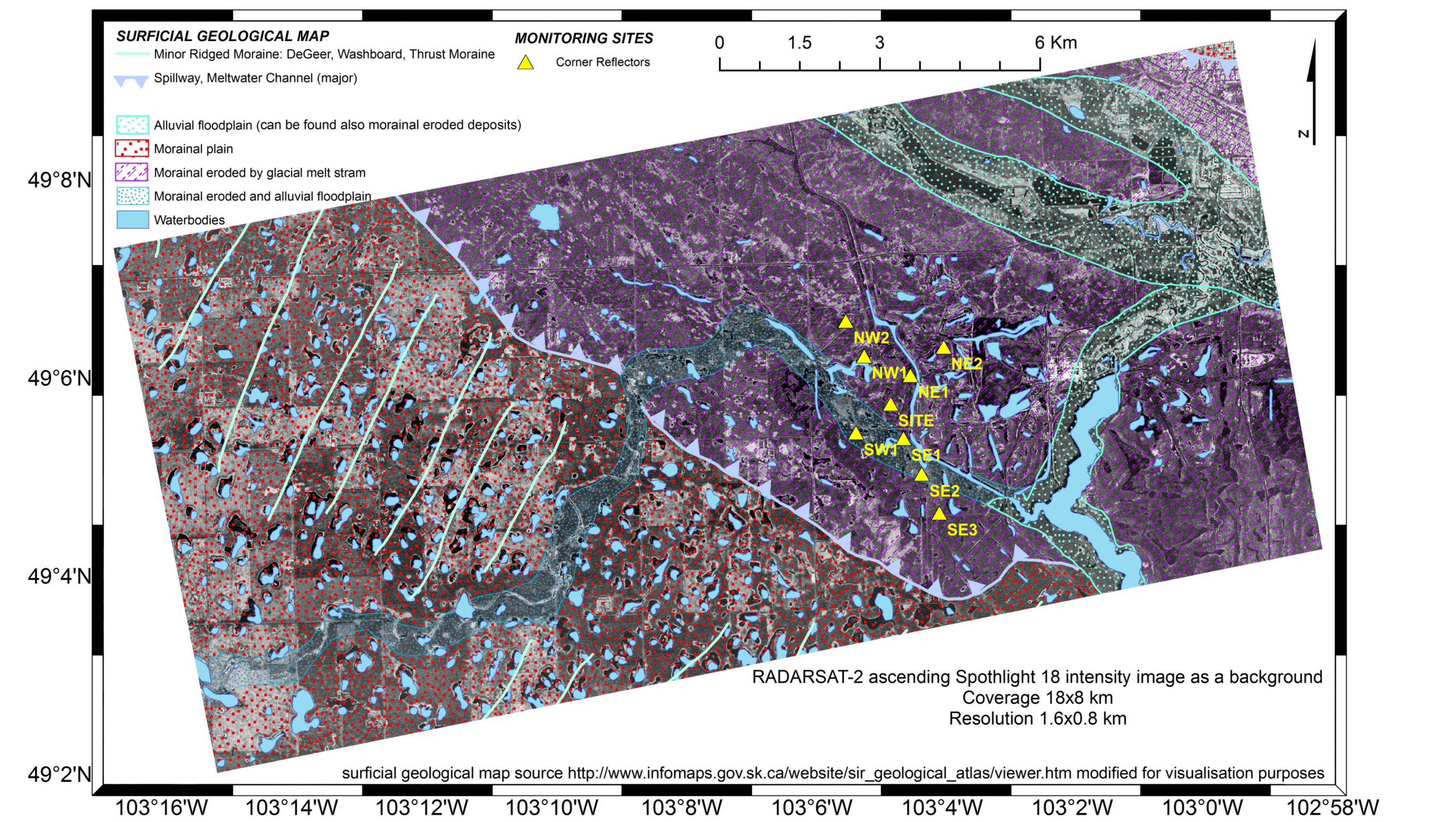

ACKNOWLEDGEMENT: We thank the Canadian Space Agency (CSA) for providing RADARSAT-2 data. Figures were plotted with GMT and Gnuplot software and R software.

REFERENCES:

[1] Costantini, M. (1998). A novel phase unwrapping method based on network programming. IEEE Transactions on Geoscience and Remote Sensing, 36 , 813-821.
[2] Goldstein, R., & Werner, C. (1998). Radar interferogram filtering for geophysical applications. Geophysical Research Letters, 25 , 4035-4038.
[3] infomaps.gov.sk.ca, (2014), http://www.infomaps.gov.sk.ca/website/sir_geological_atlas/viewer.htm
[4] Massonnet, D., & Feigl, K. (1998). Radar interferometry and its application to changes in the Earth's surface Reviews of Geophysics, 36 , 441-500.
[5] Mogi, K. (1958). Relations between the eruptions of various volcanoes and the deformation of the ground surfaces above them. University of Tokyo, Earthquake Research Institute Bulletin, 36 , 99-134
[6] Rosen, P., Hensley, P., Joughin, I., Li, F., Madsen, S., Rodriguez, E., & Goldstein, R. (2000). Synthetic aperture radar interferometry. Proceedings of the IEEE, 88 , 333-382.
[7] Samsonov, S., and d'Oreye, N., (2012). Multidimensional time series analysis of ground deformation from multiple InSAR data sets applied to Virunga Volcanic Province, Geophysical Journal International, 191, pp. 1095–1108
[8] Samsonov, S., Koij van der, M., and Tiampo, K., (2011). A simultaneous inversion for deformation rates and topographic errors of DInSAR data utilizing linear least square inversion technique, Computers & Geosciences, 37, 1083-109
[9] USGS/gdex, (2014), http://gdex.cr.usgs.gov/gdex/

Natural Resources Canada | Ressources naturelles Canada

Canada